Vector aeroacoustics for a uniform mean flow: acoustic intensity and acoustic power

Chen Xu[1,2 *], Yijun Mao[1, 2†], Zhiwei Hu[1‡]

1 University of Southampton, SO17 1BJ Southampton, United Kingdom

2 Xi'an Jiaotong University, 710049 Xi'an, People's Republic of China

and

Ghader Ghorbaniasl[3§]

3 *Vrije Universiteit Brussel (VUB), Pleinlaan 2, Brussels 1050, Belgium*

Acoustic vectors, such as acoustic velocity and acoustic intensity, have advantages over acoustic scalars in showing the detailed propagation path of acoustic energy. In this paper, acoustic vector fields around monopole and dipole sources in uniform mean flow are computed and visualized. Computational results reveal that acoustic intensity fields do not satisfy the feature of the convective amplification, and the directivity pattern of the acoustic intensity is highly dependent on the source type and the mean flow Mach number. Analytical and numerical results indicate that the acoustic power output from a monopole source is always conservative, but the acoustic power output from a dipole source is non-conservative in a uniform mean flow because there is a conversion between the acoustic energy and the vortical energy. Acoustic power output from uniformly moving sources in a quiescent acoustic medium is compared with that from the corresponding stationary sources in a uniform mean flow. The results indicate that the acoustic power output from the monopole sources is nearly the same, but the acoustic power output from the dipole sources is not equivalent in these two cases, and the deviation becomes significant with the increase in the mean flow Mach number.

[*] Research Fellow. c.xu@soton.ac.uk; xuchen1983@mail.xjtu.edu.cn.
[†] Corresponding author. y.mao@soton.ac.uk; maoyijun@mail.xjtu.edu.cn. Senior Member AIAA.
[‡] Lecturer. z.hu@soton.ac.uk. Member AIAA.
[§] Professor. ghader.ghorbaniasl@vub.ac.be.

Nomenclature

a	=	radius of the spherical surface, m
c_0	=	speed of sound in fluid, m s^{-1}
E	=	energy density, kg m^{-1} s^{-2}
f	=	data surface function
f_0	=	source pulsating frequency, Hz
G	=	frequency-domain Green's function
H	=	Heaviside function
He	=	Helmholtz number
$\mathbf{I}$	=	energy flux vector, kg m^{-2} s^{-1}
k	=	wavenumber, ω/c_0 , m^{-1}
$\mathbf{L}$	=	time-domain strength of loading source, Pa
L_M	=	$L_i M_i$, Pa
L_r	=	$L_i \hat{r}_i$, Pa
$\dot{L}_r$	=	$\frac{\partial L_i}{\partial \tau} \hat{r}_i$, Pa s^{-1}
$\hat{n}_i$	=	components of unit vector normal to the data surface
$\tilde{p}'$	=	acoustic pressure in frequency domain, Pa
Q	=	time-domain strength of thickness source, kg m^{-2} s^{-1}
r	=	geometrical distance between the source and the receiver, $\lvert\mathbf{x}-\mathbf{y}\rvert$, m
r_i	=	components of the vector in the radiation direction, $x_i - y_i$,m
$\hat{r}_i$	=	components of the unit vector in the radiation direction, r_i/r
$\tilde{\mathbf{u}}'$	=	frequency-domain fluctuating velocity, m s^{-1}
u_i	=	components of the fluid velocity, m s^{-1}
u_n	=	local normal component of the fluid velocity, m s^{-1}
v_n	=	local normal component of the data surface velocity, m s^{-1}

$\mathbf{x}$ = observer position vector, m

x_i = components of the observer position vector, m

$\mathbf{y}$ = source position vector, m

y_i = components of source position vector, m

ρ = local fluid density, kg m^{-3}

ρ_0 = fluid density of unperturbed medium, kg m^{-3}

ρ' = density perturbation, kg m^{-3}

$\delta(\cdot)$ = Dirac delta function

ω = angular frequency, rad s^{-1}

ω_0 = angular frequency of source pulsation, rad s^{-1}

Subscripts

0 = fluid variable for the unperturbed medium

a = acoustic component

L = loading source

r = vortical component

T = thickness source

x = observer quantity

y = source quantity

I. Introduction

LIGHTHILL'S pioneering work [1] has shown that the acoustic power output from a stationary quadrupole point/compact source is proportional to the eighth power of the flow Mach number. The subsequent investigations of Curle [2] as well as Ffowcs Williams and Hawkings (FW-H) [3] have indicated that the acoustic power output from stationary monopole and dipole point/compact sources is proportional to the fourth and sixth power of the flow Mach number, respectively. These investigations assume that the acoustic medium is quiescent, thus the conclusions are only approximately valid for a low-Mach-number flow. The exponential law should be corrected at high Mach numbers. However, to the best knowledge of authors, few detailed studies have been carried out so far. In a quiescent acoustic medium, the acoustic power can be computed through the integral of the square of the acoustic pressure over a closed far-field surface. However, for sound radiation in a uniform mean flow, the acoustic velocity is essential for calculating the acoustic power [4].

Moreover, the convective effect usually makes that the direction of the maximum acoustic pressure inclines upstream, and this phenomenon is generally known as convective amplification. Due to the convective amplification, researchers usually think that the acoustic energy is also prone to radiate upstream in moving fluid. Actually, the acoustic power depends not only on the acoustic pressure and the acoustic velocity but also on the mean flow velocity, thus it is still an open question of whether or how the moving fluid alters the radiation direction of the acoustic energy. Computations and visualizations of the acoustic intensity field around sources should help to address this issue. Moreover, visualizing the acoustic intensity field can reveal the detailed propagation path of the acoustic energy and the mechanism of sound propagation, thus it is beneficial to achieve an optimal noise reduction efficacy by optimizing the shape and installation location of the acoustic liner. For examples, visualization of acoustic intensity fields illustrates three modes of acoustic energy output from rotating sources [5], reveals the effect of scattering surfaces on the redistribution of the acoustic energy [6] and displays the primary acoustic-absorbing position around an impedance scattering surface [7]. All the above studies were carried out with an assumption of quiescent acoustic medium, and in this paper, the acoustic intensity field around sources as well as the acoustic power output in a uniform mean flow are investigated. The results will show that the upstream radiated acoustic power output is not always higher than the downstream radiated, and the directivity pattern is highly dependent on the source type and the mean flow Mach number.

Energy transportation of small-amplitude perturbations in moving fluid has been studied by serval researchers over the past decades. For small-amplitude perturbations in a uniform mean flow, an acoustic energy balance equation was derived from the linearized Euler equation [4, 8]. Morfey [9] extended the definition of the acoustic intensity to the case of non-uniform mean flow, after that Myers [10, 11] deduced an exact equation governing the transport of energy associated with disturbances in an arbitrary steady flow, which generalized the familiar acoustic energy equation. Especially, Atassi [12] proposed an expression of the acoustic power in an annular duct with a swirling mean flow in the high-frequency limit. All the previous studies were conducted based on the homogenous linearized Euler equation without source terms on boundary surfaces, thus the effect of source types on the acoustic power output has not been studied so far. In this paper, we analyze the acoustic output from the monopole and dipole sources in a uniform mean flow. Analytical results will show that the acoustic power output from the monopole source is conservative but that output from the dipole source is non-conservative. Numerical illustrations further validate this conclusion, and show that the non-conservative feature of the acoustic power output from the dipole source gradually becomes insignificant with the increase in the Helmholtz number, which is defined as the product of the acoustic wavenumber and the source-observer distance.

In aeroacoustics experiments, it is usually thought that sound radiated from sources in a uniform rectilinear motion, such as a moving airframe or a high-speed train, can be transformed into an equivalent case of anechoic wind tunnel in which sources are fixed in a uniform mean flow. Time-space transformation techniques, such as Galilean and Lorentz (Prandtl-Glauert) transformations [13, 14], are widely used to correlate the acoustic pressure in these two cases. However, to the best knowledge of authors, no published literature has mathematically proved that the acoustic power output in these two cases is exactly the same. Therefore, in Section IV. D of this paper, the acoustic power output in these two cases is compared for the first time.

The remaining part of this paper is organized as follows. Section II presents analytical studies on the acoustic power output from the monopole and dipole sources in a uniform mean flow, showing that the acoustic power output from the monopole is conservative but that from the dipole source is not conservative due to the conversion between the acoustic energy and vortical energy in the uniform mean flow. In Section III, the acoustic intensity fields around the monopole and dipole sources in the quiescent acoustic medium and the uniform mean flow are calculated and visualized to address the question of whether or how the moving fluid alters the radiation direction of the acoustic energy. In Section IV, acoustic power output from the monopole and dipole sources is further studied numerically

and analytically. Numerical illustrations indicate that the acoustic power output from a dipole source in the uniform mean flow is indeed not conservative. Therefore, only the analytical acoustic power formulation for a point/compact monopole source in a uniform mean flow is deduced. Based on the developed formulation, a theoretical analysis on the relationship between the acoustic power and the Mach number of the uniform mean flow is carried out. Moreover, acoustic power output from uniformly moving sources in a quiescent acoustic medium is compared with that from the corresponding stationary sources in a uniform mean flow. Finally, conclusions are drawn in Section V.

II. Fundamental analysis of acoustic energy in a uniform mean flow

We consider the small-amplitude wave propagation in an inviscid non-heat-conducting compressible fluid with solid boundaries $f=0$. Due to the inhomogeneity, the solid boundaries equivalently form a mass flow (monopole) source $Q\delta(f)$ in the continuity equation and a loading (dipole) source $\mathbf{L}\delta(f)$ in the momentum equation, where Dirac delta function $\delta(f)$ denotes that both the monopole and dipole sources are only located on the solid boundaries. Therefore, the generalized linearized continuity and Euler equations are expressed as follows:

$$\frac{\partial\left[H(f)\rho'\right]}{\partial t}+\mathbf{U}_\infty\cdot\nabla\left[H(f)\rho'\right]+\rho_0\nabla\cdot[H(f)\mathbf{u}']=Q\delta(f) \tag{1}$$

$$\rho_0\left[\frac{\partial[H(f)\mathbf{u}']}{\partial t}+\mathbf{U}_\infty\cdot\nabla[H(f)\mathbf{u}']\right]=-\nabla[H(f)p']+\mathbf{L}\delta(f) \tag{2}$$

where $\mathbf{U}_\infty$ is the velocity of uniform mean flow; ρ_0 is the density of the ambient flow; p' and $\mathbf{u}'$ are the perturbations of the static pressure and the flow velocity, respectively.

We analyze the energy transport of small-amplitude perturbations by using the following energy balance equation:

$$\frac{\partial E}{\partial t}+\nabla\cdot\mathbf{I}=S \tag{3}$$

where *E* is the energy density, $\mathbf{I}$ is the energy flux vector and the term *S* represents the energy production and conversion. Goldstein [4] constructed the terms *E* and $\mathbf{I}$ by starting from Eqs. (1) and (2), and obtained the following equations by using the assumption of $p'=\rho'c_0^2$.

$$E = H(f)\left(\frac{p'\rho'}{2\rho_0} + \frac{\rho_0 \mathbf{u}'^2}{2} + \rho' \mathbf{U}_\infty \cdot \mathbf{u}'\right) \tag{4}$$

$$\mathbf{I} = H(f)(p'/\rho_0 + \mathbf{u}' \cdot \mathbf{U}_\infty)(\rho_0 \mathbf{u}' + \rho' \mathbf{U}_\infty) \tag{5}$$

$$S = (\mathbf{u}' + \mathbf{U}_\infty \rho'/\rho_0) \cdot \mathbf{L}\delta(f) + (p'/\rho_0 + \mathbf{u}' \cdot \mathbf{U}_\infty) Q\delta(f) + H(f)\rho_0 \mathbf{U}_\infty \cdot [\boldsymbol{\omega}' \times \mathbf{u}'] \tag{6}$$

where $\boldsymbol{\omega}' = \nabla \times \mathbf{u}'$ is the instantaneous vorticity. Note that $\mathbf{u}'$ is the total perturbated velocity which consists of both the acoustic and vortical components, thus the terms E and $\mathbf{I}$ represent the total energy density and flux vector, including both the acoustic and vortical components. A similar derivation was also presented in [10] without accounting for the effect of sources on the solid boundaries. The acoustic velocity and vortical velocity are not separated in both [4] and [10], thus Eq. (3) describes the total energy transport of small-amplitude perturbations, including both the acoustic and vortical energy.

In order to describe the acoustic energy transportation, we give the following two definitions, which have a subtle difference from those defined by Goldstein [4] because the acoustic velocity $\mathbf{u}'_a$ instead of the total perturbated velocity $\mathbf{u}'$ is used:

$$\hbar = p'/\rho_0 + \mathbf{u}'_a \cdot \mathbf{U}_\infty \tag{7}$$

$$\mathbf{J} = \mathbf{u}'_a + \rho'/\rho_0 \, \mathbf{U}_\infty \tag{8}$$

Multiplying Eq. (1) by Eq. (7) and multiplying Eq. (2) by Eq.(8) give the following two equations:

$$\left[\frac{\partial[H(f)\rho']}{\partial t} + \mathbf{U}_\infty \cdot \nabla[H(f)\rho'] + \rho_0 \nabla \cdot [H(f)\mathbf{u}']\right]\left[p'/\rho_0 + \mathbf{u}'_a \cdot \mathbf{U}_\infty\right] = \hbar Q\delta(f) \tag{9}$$

$$\rho_0\left[\frac{\partial[H(f)\mathbf{u}']}{\partial t} + \mathbf{U}_\infty \cdot \nabla[H(f)\mathbf{u}']\right] \cdot \left[\mathbf{u}'_a + \rho'/\rho_0 \, \mathbf{U}_\infty\right] = \mathbf{J} \cdot \left[\mathbf{L}\delta(f) - H(f)\rho_0\left(\frac{\partial \mathbf{u}'_r}{\partial t} + \mathbf{U}_\infty \cdot \nabla \mathbf{u}'_r\right)\right] \tag{10}$$

The sum of Eq. (9) and Eq. (10) yields:

$$\frac{\partial E_a}{\partial t} + \nabla \cdot \mathbf{I}_a = S_a \tag{11}$$

with

$$E_a = H(f)\left(\frac{p'\rho'}{2\rho_0} + \frac{\rho_0 \mathbf{u}_a'^2}{2} + \rho'\mathbf{U}_\infty \cdot \mathbf{u}_a'\right) \tag{12}$$

$$\mathbf{I}_a = H(f)(p'/\rho_0 + \mathbf{u}_a' \cdot \mathbf{U}_\infty)(\rho_0 \mathbf{u}_a' + \rho'\mathbf{U}_\infty) \tag{13}$$

$$S_a = \hbar Q\delta(f) + \mathbf{J}\cdot\mathbf{L}\delta(f) - H(f)\rho_0 \mathbf{J}\cdot(\frac{\partial \mathbf{u}_r'}{\partial t} + \mathbf{U}_\infty \cdot \nabla \mathbf{u}_r') \tag{14}$$

in which the acoustic energy density E_a and acoustic intensity (acoustic energy flux) vector $\mathbf{I}_a$ are the same as those defined by Morfey [9] and Myers [10]. Three terms on the right-hand side of Eq. (14) can be interpreted as follows. The first two source terms denote the acoustic energy contributed from the dipole and monopole sources, respectively. The last term represents the acoustic-vortical interaction in a uniform mean flow.

As shown in [15], the monopole source radiates only acoustic waves but the dipole source simultaneously stimulates acoustic and vortical waves in a uniform mean flow. Therefore, we can find that the production term is $S_a = (p'/\rho_0 + \mathbf{u}_a' \cdot \mathbf{U}_\infty)Q\delta(f)$ if the perturbation is stimulated only by the monopole source in a uniform mean flow. This result means that the acoustic energy is contributed only from the monopole source, and the acoustic power output from the monopole source is always conservative. On the other hand, if the perturbation is stimulated by the dipole source in a uniform mean flow, the last term on the RHS of Eq. (14) means that the acoustic power is not conservative because there is a conversion between the acoustic energy and the vortical energy during the propagation of the acoustic and vortical waves. Some numerical illustrations will be presented in Section IV to further validate this conclusion.

By using the assumption of $p' = \rho' c_0^2$ where c_0 is the sound speed of the ambient flow, we can obtain the following frequency-domain acoustic intensity expression from Eq. (13)

$$\tilde{\mathbf{I}}_a = \frac{\tilde{p}'\tilde{\mathbf{u}}_a'^{\dagger}}{2} + \frac{\tilde{p}'\tilde{p}'^{\dagger}\mathbf{M}_\infty}{2\rho_0 c_0} + \frac{\rho_0 c_0 \tilde{\mathbf{u}}_a'(\tilde{\mathbf{u}}_a'^{\dagger}\cdot\mathbf{M}_\infty)}{2} + \frac{\tilde{p}'\mathbf{M}_\infty(\tilde{\mathbf{u}}_a'^{\dagger}\cdot\mathbf{M}_\infty)}{2} \tag{15}$$

where $H(f)$ is omitted; tilde ~ denotes frequency-domain complex quantity; superscript † denotes complex conjugation; $\mathbf{M}_\infty$ is Mach number vector of the uniform mean flow. Note that $\tilde{\mathbf{I}}_a$ is a complex vector, in which the vector represents the direction of the time-averaged acoustic intensity and the real and imaginary parts are named the

active and reactive acoustic intensity, respectively. Because the acoustic power output is contributed from the active acoustic intensity, only the active acoustic intensity field is analyzed in this paper. Since the last three terms only exist in a moving acoustic medium, Eq. (15) reduces to the conventional definition of the acoustic intensity when the acoustic medium is quiescent.

In order to properly visualize the distribution of the acoustic field around sources, the acoustic velocity and acoustic intensity levels are used to illustrate contours shown in this paper, which are defined as follows:

$$SVL = 20\log_{10}\left(\sqrt{\sum_{i=1}^{3}\left|\tilde{u}'_{a,i}\right|^2}\Big/ u_{ref}\right) \tag{16}$$

$$SIL = 10\log_{10}\left(\sqrt{\sum_{i}^{3}\mathrm{Re}\left(\tilde{I}_i\right)^2}\Big/ I_{ref}\right) \tag{17}$$

where $u_{ref} = 5\times10^{-8}\,\mathrm{m/s}$ and $I_{ref} = 10^{-12}\,\mathrm{W/m^2}$ are the reference values of the acoustic velocity and acoustic intensity, respectively. Re denotes the real part of a complex quantity.

III. Acoustic fields around sources in a uniform mean flow

A. Acoustic fields around stationary sources in a uniform mean flow

It is assumed that the stationary sources are located at the origin of the coordinate system and the uniform mean flow is along the positive *z*-axis direction. Computations are performed for the monopole and dipole sources in the quiescent acoustic medium and the uniform mean flow with a Mach number of 0, 0.4 and 0.8, respectively. In the following figures, the black solid line, blue dashed line and red dashed dot line are used to represent the cases of $M_\infty = 0$, $M_\infty = 0.4$ and $M_\infty = 0.8$, respectively. The source strength of the monopole point source is $\int_{f=0} \tilde{Q}^M dS = 0.01\,\mathrm{kg\cdot s^{-1}}$. Since the irrotational and solenoidal components of a dipole source stimulate acoustic and vortical waves in uniform mean flow [15], respectively, here we only analyze sound radiated from the irrotational component. For the stationary dipole source, it is assumed that the irrotational component of the dipole source strength is $\int_{f=0} \tilde{\mathbf{L}}_a^M dS = (0,0,1)\,\mathrm{N}$ and $\int_{f=0} \tilde{\mathbf{L}}_a^M dS = (0,1,0)\,\mathrm{N}$, respectively, in order to analyze the effect

of the relationship between the flow direction and the dipole axis direction on sound radiation. In all numerical test cases, the source-pulsating frequency is $f_0 = 100\,\mathrm{Hz}$.

Frequency-domain acoustic pressure and acoustic velocity are computed numerically by using the following equations [15, 16]:

$$H(f)4\pi \tilde{p}'_T(\mathbf{x},\omega) = -\int_{f=0} \frac{\mathrm{i}kc_0\tilde{Q}^M\left(1-M_{\infty R}\right)}{R^*}\mathrm{e}^{\mathrm{i}kR}\mathrm{d}S - \int_{f=0}\frac{c_0\tilde{Q}^M M_{\infty R^*}}{R^{*2}}\mathrm{e}^{\mathrm{i}kR}\mathrm{d}S \tag{18}$$

$$H(f)4\pi \tilde{p}'_L(\mathbf{x},\omega) = -\int_{f=0} \frac{ik\tilde{L}^M_{a,R}}{R^*}\mathrm{e}^{\mathrm{i}kR}\mathrm{d}S + \int_{f=0}\frac{\tilde{L}^M_{a,R^*}}{R^{*2}}\mathrm{e}^{\mathrm{i}kR}\mathrm{d}S \tag{19}$$

$$H(f)4\pi\rho_0\tilde{u}'_{a,Ti}(\mathbf{x},\omega) = -\int_{f=0} \frac{\mathrm{i}k\tilde{Q}^M\hat{R}_i}{R^*}\mathrm{e}^{\mathrm{i}kR}\mathrm{d}S + \int_{f=0}\frac{\tilde{Q}^M\hat{R}^*_i}{R^{*2}}\mathrm{e}^{\mathrm{i}kR}\mathrm{d}S \tag{20}$$

$$\begin{aligned} H(f)4\pi\rho_0 c_0\tilde{u}'_{a,Li}(\mathbf{x},\omega) = -\mathrm{i}k &\int_{f=0}\frac{\tilde{L}^M_{a,R}\hat{R}_i + \left(M_{\infty R} - M^2_{\infty R}\right)\tilde{L}^M_{a,i}}{R^*}e^{\mathrm{i}kR}\mathrm{d}S \\ &+\int_{f=0}\frac{\tilde{L}^M_{a,R^*}\hat{R}_i + \left(\tilde{L}_{a,R} + \gamma^2\tilde{L}_{a,R^*}\right)\hat{R}^*_i - \tilde{L}^M_{a,i}}{R^{*2}}e^{\mathrm{i}kR}\mathrm{d}S \\ &+\int_{f=0}\frac{\left(M_{\infty R^*} - 2M_{\infty R}M_{\infty R^*} + \gamma^2M^2_\infty - \gamma^2M^2_{\infty R^*}\right)\tilde{L}^M_{a,i} - \gamma^2\tilde{L}^M_{a,M_\infty}M_{\infty i}}{R^{*2}}e^{\mathrm{i}kR}\mathrm{d}S \\ &+\frac{\mathrm{i}}{k}\int_{f=0}\frac{3\tilde{L}^M_{a,R^*}\hat{R}^*_i + \left(2M^2_\infty - 3M^2_{\infty R^*} - 1\right)\tilde{L}^M_{a,i} - \tilde{L}^M_{a,M_\infty}M_{\infty i}}{R^{*3}}e^{\mathrm{i}kR}\mathrm{d}S \end{aligned} \tag{21}$$

where subscript *T* and *L* represent the values related to the thickness and loading sources, respectively; subscripts *i* and *j* mean the i^{th} and j^{th} directions, respectively; ω is the angular frequency; *k* is the wavenumber; $M_{\infty R^*} = M_{\infty j}\hat{R}^*_j$; $\tilde{L}^M_{a,R} = \tilde{L}^M_{a,j}\hat{R}_j$; $\tilde{L}^M_{a,R^*} = \tilde{L}^M_{a,j}\hat{R}^*_j$ (see detailed expressions in [15, 16]). Note that the first term on the right-hand side (RHS) of the above equations is named far-field term which will be used to deduce the analytical acoustic power formulation in Section IV.

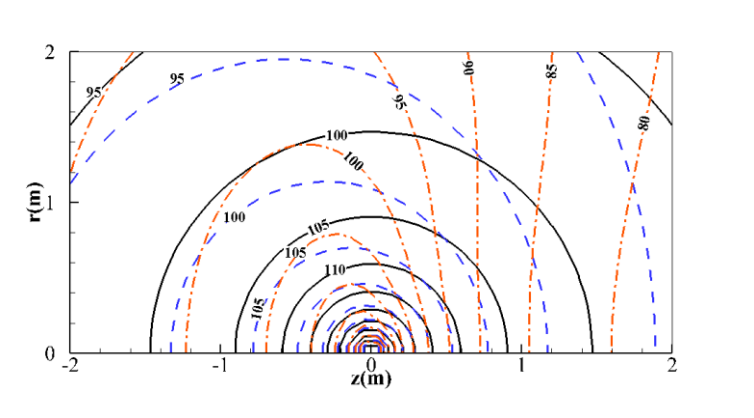

Fig. 1 Acoustic velocity field around a stationary monopole point source

Since the acoustic field is axisymmetric around the z axis, a cylindrical coordinate system (r,θ,z) is also used in the following analysis, in which the relationships $r=\sqrt{x^2+y^2}$ and $\theta=\cos^{-1}(x/r)$ are used to transfer the coordinates in these two coordinate systems. Fig. 1 illustrates that the acoustic velocity field around the monopole source in the quiescent acoustic medium and the uniform mean flow, respectively. The mean flow makes the maximum acoustic velocity is prone to the upstream direction, thus the convective amplification can be observed in the acoustic velocity field.

Fig. 2 displays the acoustic intensity field around the stationary monopole source, where the contour denotes the acoustic intensity level and the vector on the acoustic energy streamlines [17, 18] indicates the direction of the active acoustic intensity. An interesting and important phenomenon is that, regardless of the uniform mean flow, the acoustic intensity field upstream and downstream of the monopole source is always symmetric. This distribution feature of the acoustic intensity field is greatly different from that of the acoustic pressure and the acoustic velocity fields. Fig. 2 also indicates that the uniform mean flow increases the acoustic intensity on the plane perpendicular to the flow direction. The higher the flow Mach number is, the more percentages of the acoustic energy concentrate on the plane of z=0. Moreover, the acoustic energy streamlines shown in Fig. 2 indicate that the propagation path of acoustic energy output from the stationary monopole source is invariant with the flow Mach number.

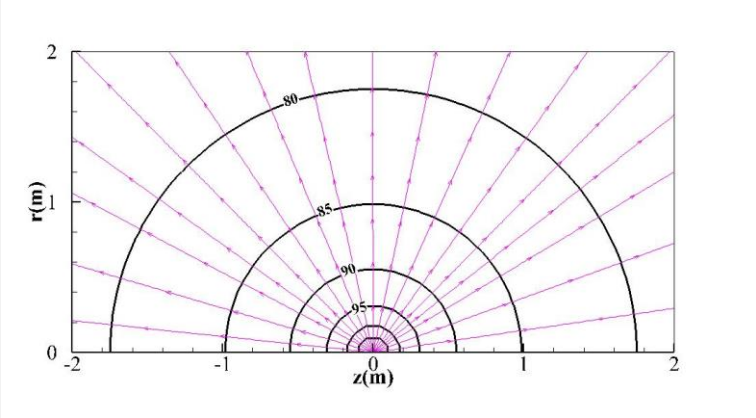

(a)

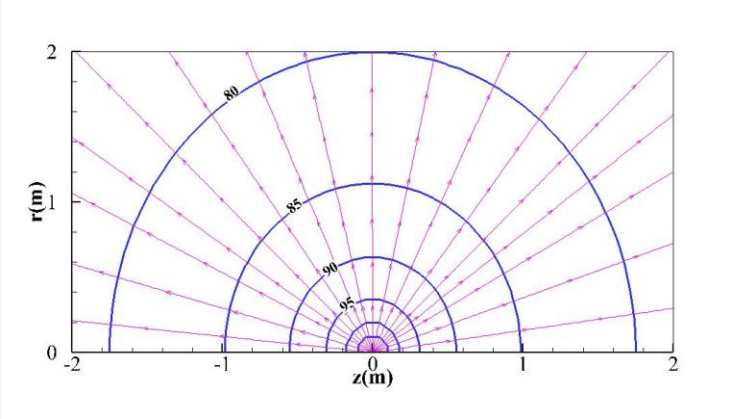

(b)

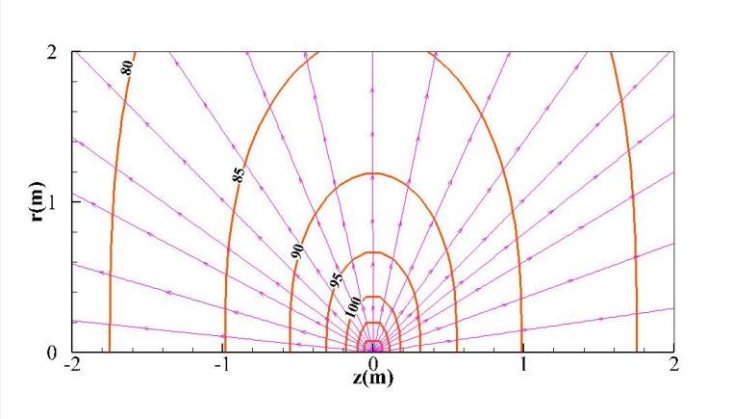

(c)

Fig. 2 Acoustic intensity field and acoustic energy streamlines around a stationary monopole point source: (a) $M_\infty = 0$**; (b)** $M_\infty = 0.4$**; (c)** $M_\infty = 0.8$

For a dipole source with its axis in the same direction as the uniform mean flow, the acoustic velocity and acoustic intensity fields are illustrated in Fig. 3 and Fig. 4, respectively. Fig. 5 and Fig. 6 illustrate the acoustic fields for a dipole source whose axis is perpendicular to the uniform mean flow. When the dipole axis has the same direction as the mean flow, the fields of the acoustic velocity and acoustic intensity are asymmetric owing to the

convective amplification. However, when the dipole axis is perpendicular to the mean flow, the acoustic fields do not always satisfy the feature of the convective amplification. Both the acoustic velocity and acoustic intensity fields are asymmetric, but the directivity pattern of the acoustic intensity is highly dependent on the flow Mach number. For example, Fig. 6(c) shows that the maximum acoustic intensity inclines upstream but Fig. 6(b) shows that the maximum acoustic intensity inclines downstream.

Compared with the monopole source, the acoustic fields around the dipole sources in a uniform mean flow are much more complex. As shown in Fig. 2, the arrows are always outward from the monopole source either in the quiescent acoustic medium or in the uniform mean flow, but the arrows shown in Fig. 4(b), (c) and Fig. 6 (b), (c) illustrate that the dipole source radiates a part of acoustic energy as well as absorbs simultaneously another part of acoustic energy.

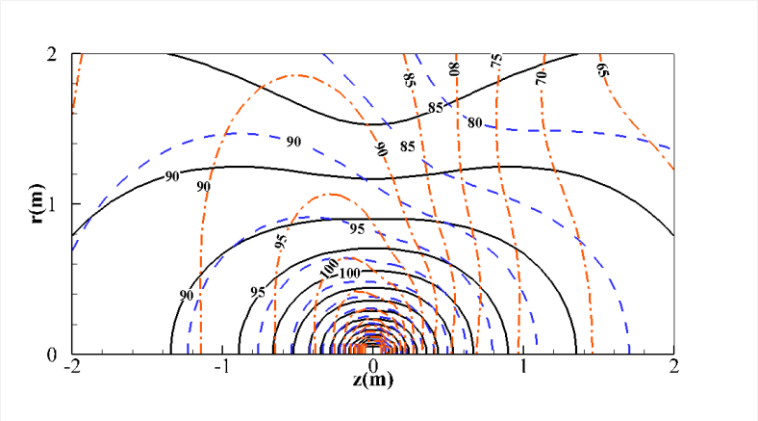

Fig. 3 Acoustic velocity field around a stationary dipole point source $\mathbf{L}_a = (0,0,1)\,\mathrm{N}$

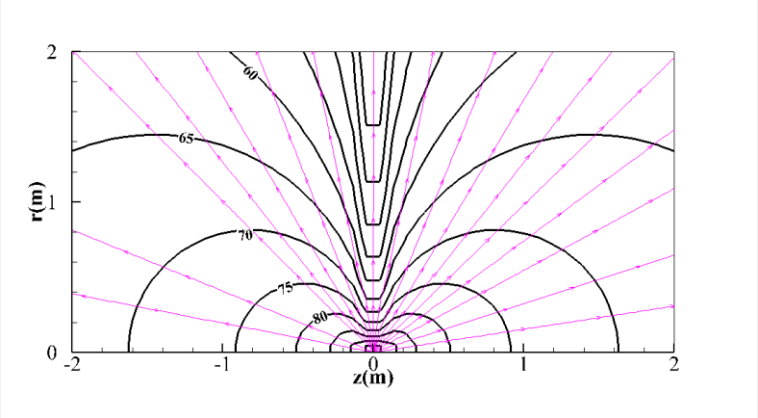

(a)

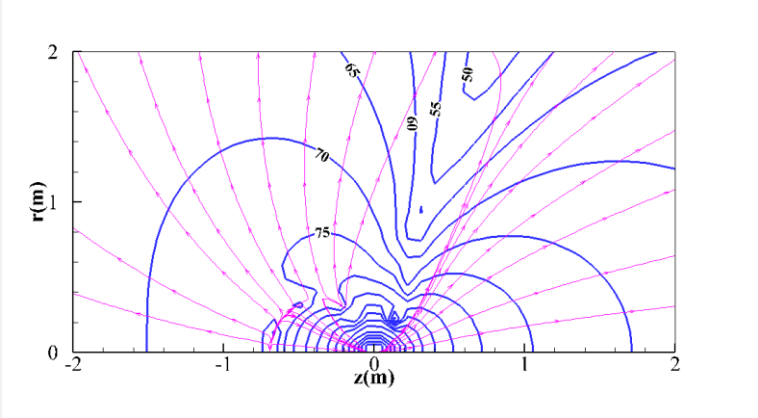

(b)

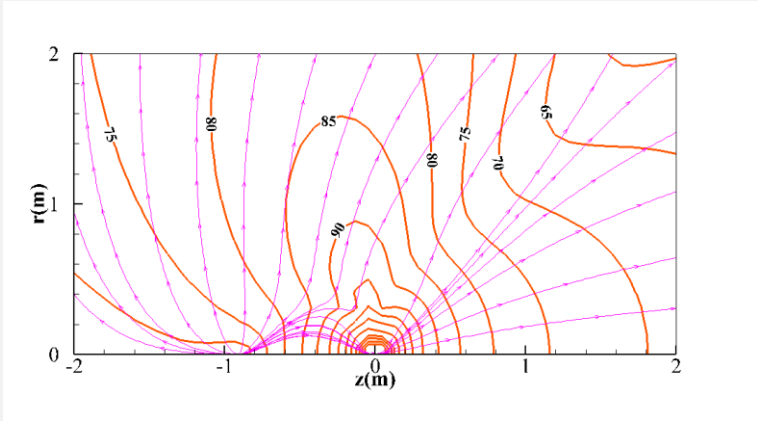

(c)

Fig. 4 Acoustic intensity field and acoustic energy streamlines around a stationary dipole point source $\mathbf{L}_a = (0,0,1)\,\mathrm{N}$: **(a)** $M_\infty = 0$; **(b)** $M_\infty = 0.4$; **(c)** $M_\infty = 0.8$.

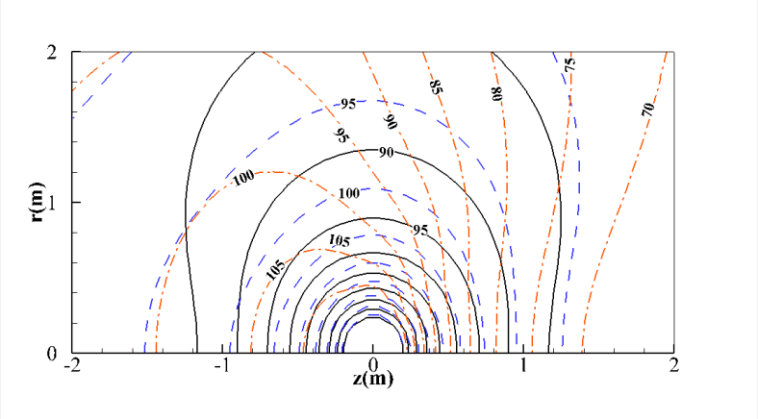

Fig. 5 Acoustic velocity field around a stationary dipole point source $\mathbf{L}_a = (0,1,0)\,\mathrm{N}$

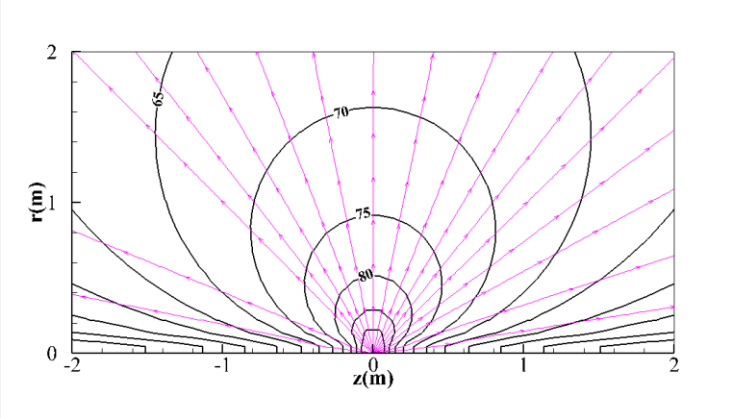

(a)

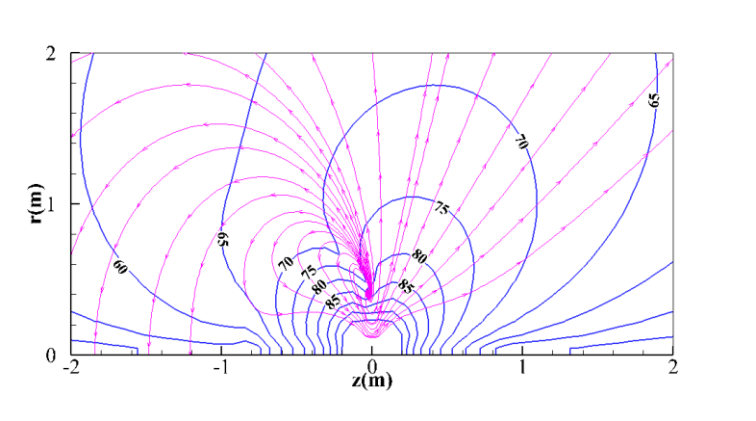

(b)

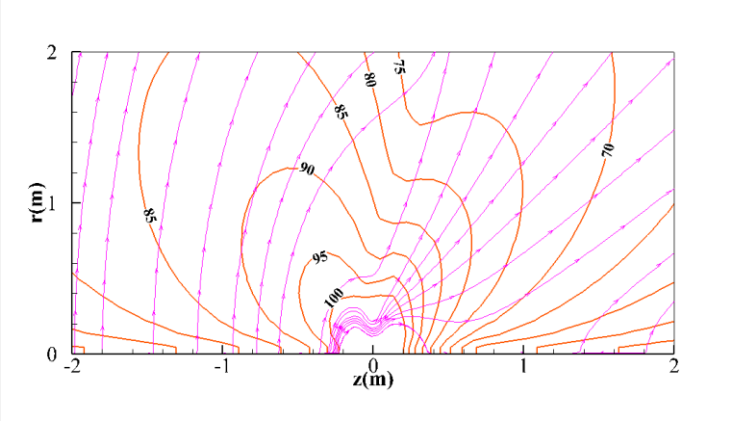

(c)

Fig. 6 Acoustic intensity field around a stationary dipole point source $\mathbf{L}_a = (0,1,0)\,\mathrm{N}$: (a) $M_\infty = 0$; (b) $M_\infty = 0.4$; (c) $M_\infty = 0.8$.

B. Acoustic fields around rotating sources in a uniform mean flow

In this subsection, we analyze the acoustic fields around rotating monopole and dipole point sources. The sources rotate around the *z* axis in the plane of *z*=0 with the radius of rotation of 0.8m, and the frequency of the

source rotation and the source pulsation is 50Hz and 100Hz, respectively. The acoustic fields around the rotating sources in the quiescent acoustic medium and the uniform mean flow are calculated, respectively. The uniform mean flow is along the positive *z* direction, and the flow Mach numbers tested are 0.4 and 0.8, respectively. Tonal noise with discrete frequencies radiates from a rotating source with a constant angular speed, and we only compute the component at the frequency of 50Hz in this paper.

For the rotating monopole and dipole sources either in the quiescent acoustic medium or in the uniform mean flow, frequency-domain acoustic pressure and acoustic velocity are computed with the following integral formulations [15, 16]:

$$H(f)4\pi \tilde{p}'_T(\mathbf{x},\omega) = -\int_{-\infty}^{\infty}\int_{f=0} \frac{\mathrm{i}kc_0 Q^M\left(1-M_{\infty R}\right)}{R^*}\mathrm{e}^{\mathrm{i}kR}\mathrm{e}^{\mathrm{i}\omega\tau}\mathrm{d}S\mathrm{d}\tau - \int_{-\infty}^{\infty}\int_{f=0} \frac{c_0 Q^M M_{\infty R^*}}{R^{*2}}\mathrm{e}^{\mathrm{i}kR}\mathrm{e}^{\mathrm{i}\omega\tau}\mathrm{d}S\mathrm{d}\tau \quad (22)$$

$$H(f)4\pi \tilde{p}'_L(\mathbf{x},\omega) = -\int_{-\infty}^{\infty}\int_{f=0} \frac{ikL^M_{a,R}}{R^*}\mathrm{e}^{ikR}\mathrm{e}^{i\omega\tau}\mathrm{d}S\mathrm{d}\tau + \int_{-\infty}^{\infty}\int_{f=0} \frac{L^M_{a,R^*}}{R^{*2}}\mathrm{e}^{ikR}\mathrm{e}^{i\omega\tau}\mathrm{d}S\mathrm{d}\tau \quad (23)$$

$$H(f)4\pi\rho_0\tilde{u}'_{a,Ti}(\mathbf{x},\omega) = \int_{-\infty}^{\infty}\int_{f=0}\left[-\frac{\mathrm{i}\,kQ^M\hat{R}_i}{R^*} + \frac{Q^M\hat{R}_i^*}{R^{*2}}\right]\mathrm{e}^{\mathrm{i}kR}\mathrm{e}^{\mathrm{i}\omega\tau}\mathrm{d}S\mathrm{d}\tau \quad (24)$$

$$\begin{aligned}
H(f)4\pi\rho_0\tilde{u}'_{a,Li}(\mathbf{x},\omega) = -\mathrm{i}k\int_{-\infty}^{\infty}\int_{f=0} & \frac{L^M_{a,R}\hat{R}_i + \left(M_{\infty R} - M^2_{\infty R}\right)L^M_{a,i}}{c_0 R^*}e^{\mathrm{i}kR}e^{\mathrm{i}\omega\tau}\mathrm{d}S\mathrm{d}\tau \\
+\int_{-\infty}^{\infty}\int_{f=0} & \frac{L^M_{a,R^*}\hat{R}_i + \left(L^M_{a,R} + \gamma^2 L^M_{a,R^*}\right)\hat{R}_i^* - L^M_{a,i}}{c_0 R^{*2}}e^{\mathrm{i}kR}e^{\mathrm{i}\omega\tau}\mathrm{d}S\mathrm{d}\tau \\
+\int_{-\infty}^{\infty}\int_{f=0} & \frac{\left(M_{\infty R^*} - 2M_{\infty R}M_{\infty R^*} + \gamma^2 M^2_{\infty} - \gamma^2 M^2_{\infty R^*}\right)L^M_{a,i} - \gamma^2 L^M_{a,M_\infty}M_{\infty i}}{c_0 R^{*2}}e^{\mathrm{i}kR}e^{\mathrm{i}\omega\tau}\mathrm{d}S\mathrm{d}\tau \\
+\frac{\mathrm{i}}{k}\int_{-\infty}^{\infty}\int_{f=0} & \frac{3L^M_{a,R^*}\hat{R}_i^* + \left(2M^2_{\infty} - 3M^2_{\infty R^*} - 1\right)L^M_{a,i} - L^M_{a,M_\infty}M_{\infty i}}{c_0 R^{*3}}e^{\mathrm{i}kR}e^{\mathrm{i}\omega\tau}\mathrm{d}S\mathrm{d}\tau
\end{aligned} \quad (25)$$

where the source strength of the monopole point source is $\int_{f=0}\tilde{Q}^M dS = 0.01\mathrm{kg}\cdot\mathrm{s}^{-1}$; the source strength of the dipole source expressed in a cylindrical coordinate system is $\int_{f=0}\tilde{L}^M_{a,j} = 1N,\ j = r,\theta,z$. The acoustic fields around the rotating dipole source with three different directions of the dipole axis are calculated, respectively.

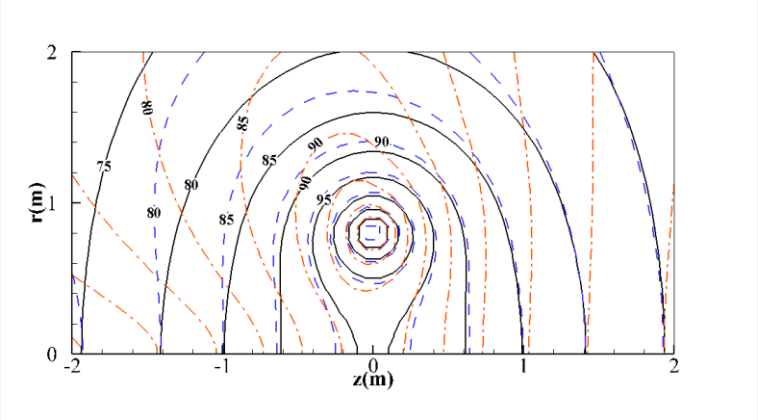

Fig. 7 Acoustic velocity field around a rotating monopole point source

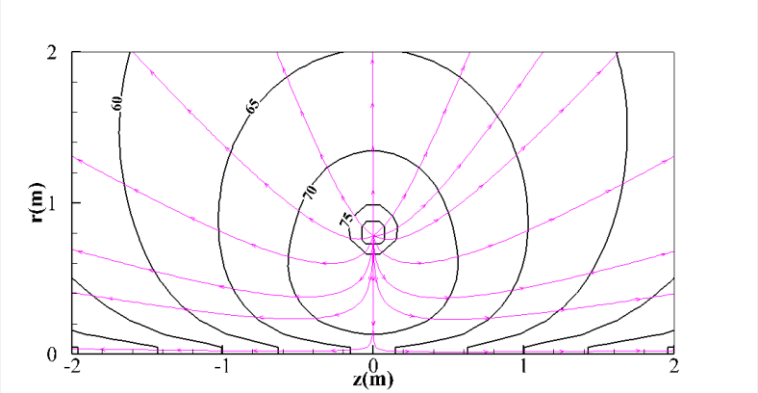

(a)

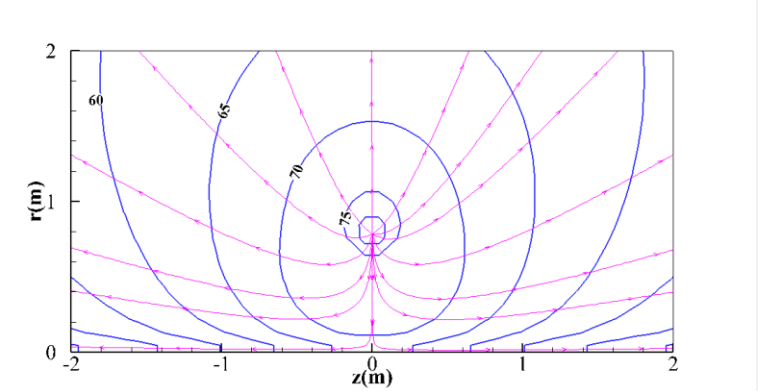

(b)

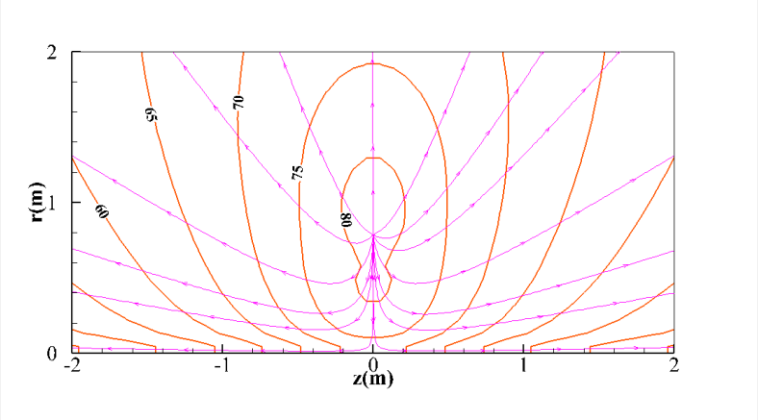

(c)

Fig. 8 Acoustic intensity field and acoustic energy streamlines around a rotating monopole source: (a) $M_\infty = 0$**; (b)** $M_\infty = 0.4$**; (c)** $M_\infty = 0.8$

Fig. 7 displays the acoustic velocity field around the rotating monopole source, showing that the direction of the maximum acoustic velocity inclines upstream in the uniform mean flow. The acoustic intensity field around the rotating monopole source is displayed in Fig. 8. Computational results indicate that the acoustic intensity field around the rotating monopole source in the uniform mean flow is symmetrical to the plane of source rotation. The proportion of the acoustic energy concentrating on the plane of source rotation increases with the flow Mach number, but the flow Mach number has no effect on the acoustic energy streamlines.

Therefore, the stationary and rotating monopole sources in the uniform mean flow have the same radiation features as follows. Firstly, both the acoustic pressure and acoustic velocity fields satisfy the feature of the convective amplification. Secondly, the acoustic intensity field is always symmetric and the proportion of the acoustic energy concentrating on the plane perpendicular to the flow direction increases with the flow Mach number. Thirdly, the mean flow cannot alter the propagation path of the acoustic energy.

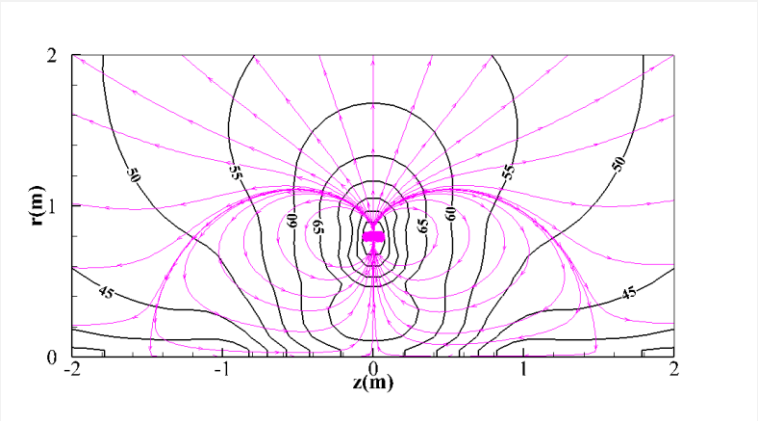

(a)

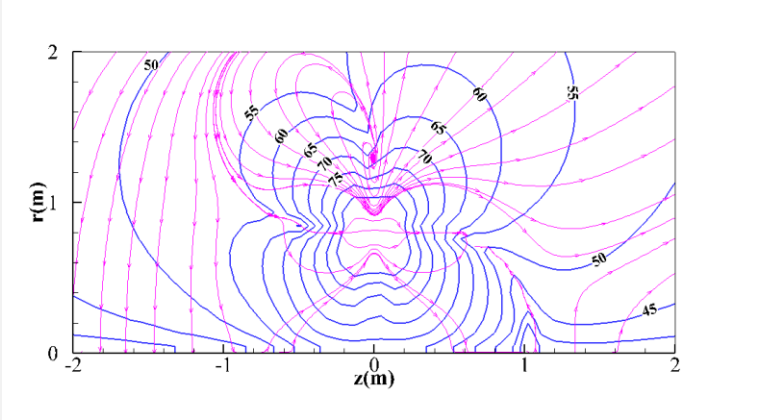

(b)

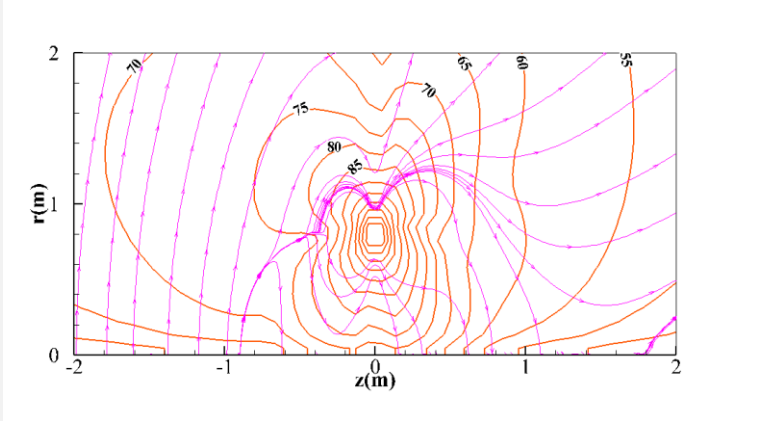

(c)

Fig. 9 Active acoustic intensity field and acoustic energy streamlines around a rotating radial dipole source: (a) $M_\infty = 0$; **(b)** $M_\infty = 0.4$; **(c)** $M_\infty = 0.8$

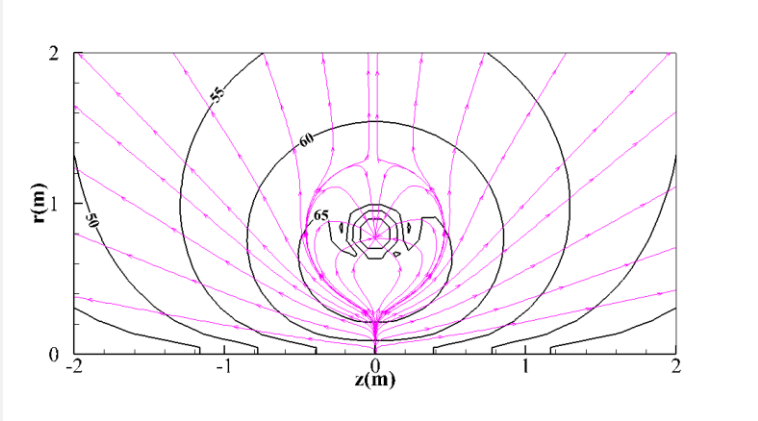

(a)

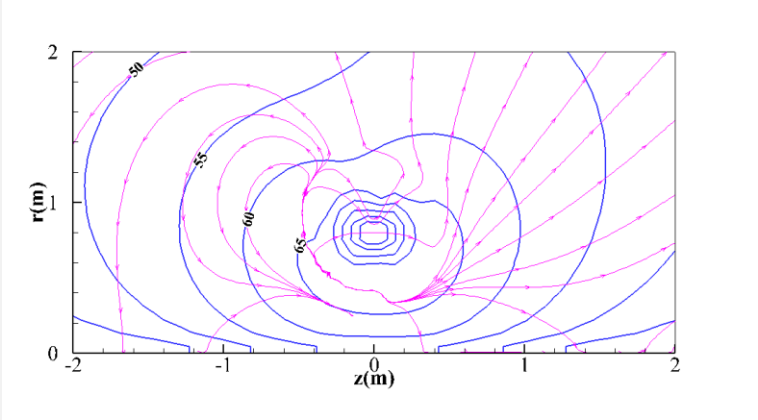

(b)

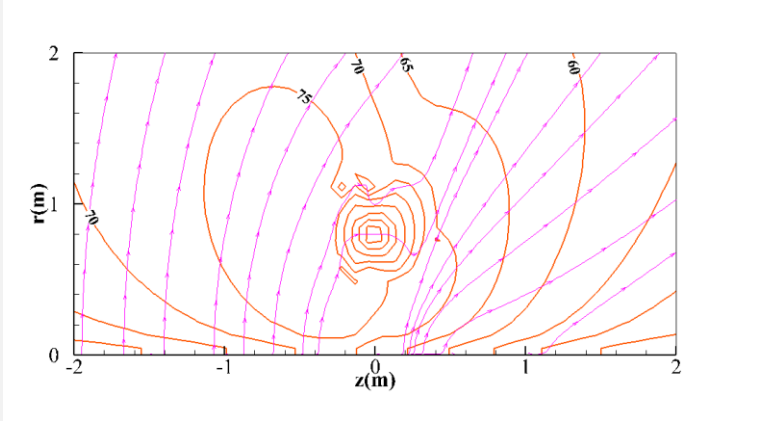

(c)

Fig. 10 Active acoustic intensity field and acoustic energy streamlines around rotating circumferential dipole source: (a) $M_\infty = 0$**; (b)** $M_\infty = 0.4$**; (c)** $M_\infty = 0.8$

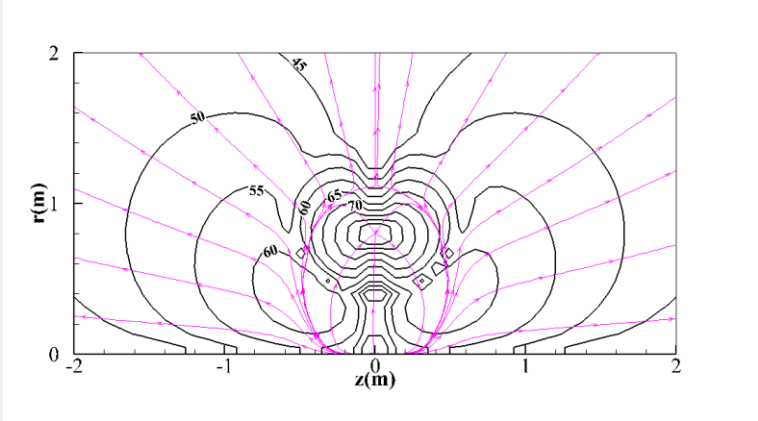

(a)

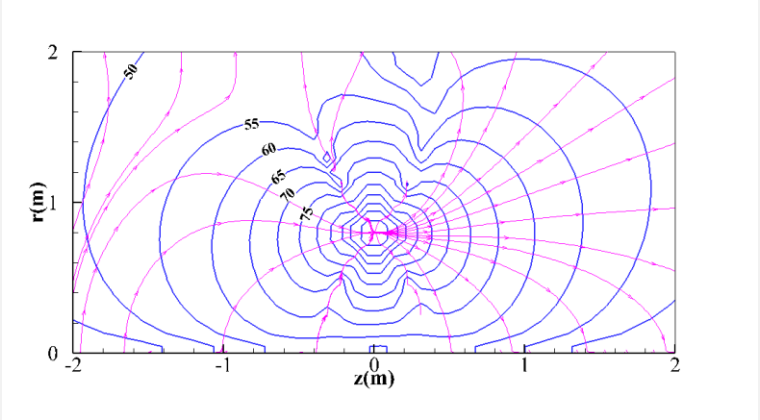

(b)

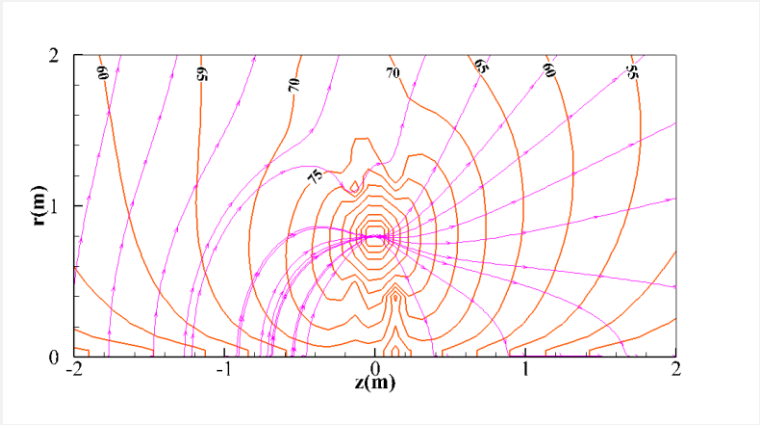

(c)

Fig. 11 Active acoustic intensity field and acoustic energy streamlines around rotating axial dipole source: (a) $M_\infty = 0$; **(b)** $M_\infty = 0.4$; **(c)** $M_\infty = 0.8$

The acoustic intensity fields around the rotating dipole sources are illustrated in Fig. 9-Fig. 11. Similar to the cases of the stationary dipole sources, the acoustic intensity fields around the rotating dipole sources are asymmetric in the uniform mean flow, but do not satisfy the feature of the convective amplification. For example, Fig. 10(b) shows that the acoustic intensity downstream the source is higher than that upstream the source.

Based on all the above computational results, we can conclude that the acoustic intensity fields around the monopole and dipole sources either at rest or in rotation do not satisfy the feature of the convective amplification. The acoustic intensity field around the monopole source is always symmetric, and the mean flow does not alter the propagation path of the acoustic energy. The acoustic intensity field around the dipole source is asymmetric, and the directivity pattern is highly dependent on the mean flow Mach number and the direction of the dipole axis. The complexity of the acoustic intensity field in the uniform mean implies that the acoustic liner should be designed carefully to attenuate the noise as much as possible.

IV. Acoustic power output from sources in a uniform mean flow

A. Definitions of acoustic power and acoustic power ratio

The acoustic power is computed by

$$W = \int_{\Gamma} \mathrm{Re}(\tilde{\mathbf{I}}_a \cdot \mathbf{n}) d\Gamma \tag{26}$$

where Γ is a closed integral surface of observers, $\mathbf{n}$ is the unit vector normal to the surface Γ, $\tilde{\mathbf{I}}_a$ is the frequency-domain active acoustic intensity defined in Eq. (15), Re denotes the real part of a complex quantity. In order to simplify the analysis, we assume that the compact/point source is located at the origin of the coordinate system and the uniform mean flow is along the positive *z* direction. A spherical surface is selected as the integral surface Γ, and its centre is located at the origin of the coordinate system. Based on this definition, Eq. (26) can be equivalently expressed as

$$W = 2\pi r^2 \int_0^{\pi} \mathrm{Re}(\tilde{I}_{a,r}) \sin\theta d\theta \tag{27}$$

where $\tilde{I}_{a,r} = \tilde{I}_{a,i}\hat{r}_i$, $\hat{r}_i = r_i / r$ and θ is the inclination angle between the positive *z* axis and the position vector of the observer. Furthermore, we can obtain the following identities which can be used in the following derivation:

$$R^* = \frac{\sqrt{r^2 + \gamma^2 (\mathbf{M}_{\infty} \cdot \mathbf{r})^2}}{\gamma} = r\sqrt{1 - M_{\infty}^2 \sin^2\theta} \tag{28}$$

$$R = \gamma^2 \left(R^* - r M_{\infty r} \right) = \frac{r\left(\sqrt{1 - M_{\infty}^2 \sin^2\theta} - M_{\infty} \cos\theta \right)}{1 - M_{\infty}^2} \tag{29}$$

$$1 - M_{\infty R} = \frac{\sqrt{1 - M_{\infty}^2 \sin^2\theta} - M_{\infty} \cos\theta}{(1 - M_{\infty}^2)\sqrt{1 - M_{\infty}^2 \sin^2\theta}} > 0 \tag{30}$$

$$\hat{R}_i \hat{r}_i = \frac{\sqrt{1 - M_{\infty}^2 \sin^2\theta} - M_{\infty} \cos\theta}{1 - M_{\infty}^2} > 0 \tag{31}$$

with $\gamma = \sqrt{1 / \left(1 - M_{\infty}^2\right)}$.

A non-dimensional parameter, acoustic power ratio (APR), was defined in previous studies [19, 20] to analyze the effect of source motion on acoustic power output. Here, a similar definition is employed to analyze the effect of uniform mean flow on the acoustic power output as follows:

$$\sigma = \frac{W_{M_\infty}}{W_0} = \sum_{n=1}^{4} W_{M_\infty,n} \Big/ W_0 \tag{32}$$

where subscripts M_∞ and 0 represent the uniform mean flow and the quiescent acoustic medium, respectively; $W_{M_\infty,n}$ represents the component of the acoustic power contributed from the *n*th term on the RHS of Eq. (15).

Based on this definition, the acoustic power level is computed by

$$\mathrm{SWL}_{M_\infty} = \mathrm{SWL}_0 + 10\log_{10}(\sigma) \tag{33}$$

where the term $10\log_{10}(\sigma)$ can be regarded as the correction of the acoustic power level accounting for the uniform mean flow.

B. Numerical computation of acoustic power output from sources

The acoustic power output from the stationary monopole and dipole point sources is computed with the numerical integral method in this subsection. The stationary source is located at the origin of the coordinate system, and the strengths of the monopole and dipole sources are $\int_{f=0} \tilde{Q}^M dS = 0.01\,\mathrm{kg}\cdot\mathrm{s}^{-1}$ and $\int_{f=0} \tilde{\mathbf{L}}_a^M dS = (1,1,1)\,\mathrm{N}$. The angular frequency of the source pulsation is $\omega_0 = 10\,\mathrm{rad}\cdot\mathrm{s}^{-1}$. For the quiescent acoustic medium and the uniform mean flow with different Mach numbers of 0.4 and 0.8, the acoustic power through spherical surfaces with different radii *a*=1m, 2m, 3m, 4m, and 5m is computed, respectively. All the spherical surfaces have the same centre locating at the origin of the coordinate system, and each spherical surface is evenly discretized into 863 elements. A non-dimensional Helmholtz parameter is defined by $\mathrm{He} = \omega_0 a / c_0$ to correlate the acoustic wavelength with the propagation distance.

Fig. 12 and Fig. 13 display the acoustic power output from the monopole and dipole sources, respectively. Fig. 12 shows that the acoustic power output from the monopole source is independent of the Helmholtz number,

indicating the acoustic power is always conservative for the sound radiation from the monopole source. In Fig. 13, the acoustic power output from the dipole source is also independent of the Helmholtz number when the Mach number is zero, but the acoustic power output gradually decreases with the increase of the Helmholtz number in the uniform mean flow. This feature is explained as follows. The dipole source only radiates acoustic waves in the quiescent acoustic medium, thus the acoustic power is always conservative during the propagation without considering the effect of fluid viscosity. However, in the uniform mean flow, the dipole source simultaneously stimulates acoustic and vortical waves [15], Eq. (14) clearly indicates that there is an energy conversion between the acoustic wave and the vortical wave, thus the acoustic power output from the dipole source is non-conservative in the uniform mean flow, as shown in Fig. 13. Moreover, Fig. 13 also indicates that the acoustic power loss becomes gradually insignificant at high Helmholtz numbers (i.e., high frequency sound in the acoustic far field). This conclusion is similar to that drawn by Atassi [12] who analyzed the acoustic energy propagation in a steady swirling flow.

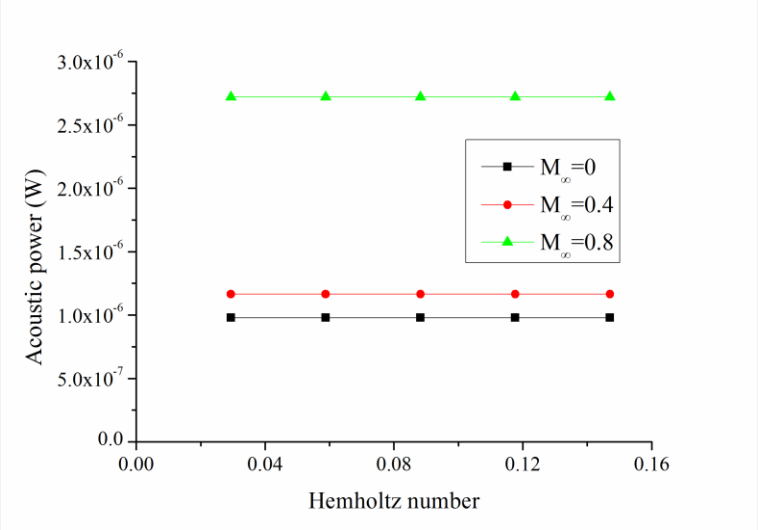

Fig. 12 Acoustic power output from a stationary monopole point source

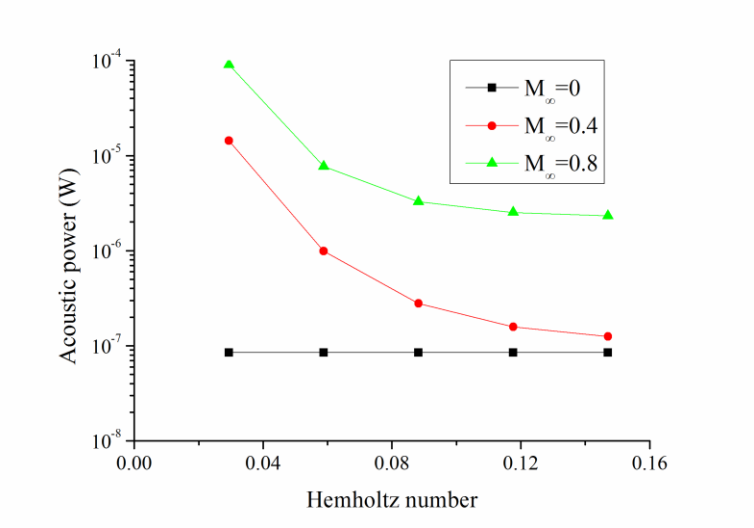

Fig. 13 Acoustic power output from a stationary dipole point source

C. Acoustic power ratio of a stationary monopole source

We consider the acoustic power output from a stationary monopole point source. This model was employed by Ffowcs Williams and Lovely [21] to analyze sound radiation from a vibrating compact surface in a uniform mean flow, assuming the monopole source strength in the uniform mean flow is the same as that in the quiescent acoustic medium and ignoring sound radiated from the force acting on the vibrating surface [22].

Since sound radiation from a monopole source is lossless in the inviscid acoustic medium, the acoustic power is independent of the integral surface Γ. Here, we define a spherical surface with a large enough radius as the integral surface Γ. An advantage of this treatment is that only the contribution from the far-field term needs to be considered for calculating the acoustic power.

As shown in Eqs. (18) and (20), the far-field terms of the frequency-domain acoustic pressure and acoustic velocity formulations for a stationary monopole source in the uniform mean flow are as follows:

$$H(f)4\pi\tilde{p}'_T(\mathbf{x},\omega) = -\int_{f=0} \frac{\mathrm{i}kc_0\tilde{Q}^M(1-M_{\infty R})}{R^*}\mathrm{e}^{\mathrm{i}kR}\mathrm{d}S, \quad |\mathbf{x}-\mathbf{y}| \to \infty \tag{34}$$

$$H(f)4\pi\rho_0\tilde{u}'_{Ti}(\mathbf{x},\omega) = -\int_{f=0} \frac{\mathrm{i}k\tilde{Q}^M\hat{R}_i}{R^*}\mathrm{e}^{\mathrm{i}kR}\mathrm{d}S, \quad |\mathbf{x}-\mathbf{y}| \to \infty \tag{35}$$

In order to simplify the following derivation, the assumption of an acoustically compact/point source is used to eliminate the surface integral sign in the following results. Substituting Eqs. (34) and (35) into Eq. (27) and employing Eqs. (28)-(31) give the following results

$$\begin{aligned} W_{M_\infty,1} &= \frac{\omega^2 \left|\tilde{Q}^M\right|^2 r^2}{16\pi\rho_0 c_0} \int_0^\pi \frac{(1-M_{\infty R})\hat{R}_i \hat{r}_i}{R^{*2}} \sin\theta d\theta \\ &= \underbrace{\frac{\omega^2 \left|\tilde{Q}^M\right|^2}{8\pi\rho_0 c_0}}_{W_0} \underbrace{\frac{2\,\mathrm{arctanh}(M_\infty) - M_\infty}{M_\infty (1-M_\infty^2)^2}}_{\sigma_1} \end{aligned} \tag{36}$$

$$\begin{aligned} W_{M_\infty,2} &= \frac{\omega^2 \left|\tilde{Q}^M\right|^2 r^2}{16\pi\rho_0 c_0} \int_0^\pi \frac{(1-M_{\infty R})^2}{R^{*2}} M_\infty \sin^2\theta d\theta \\ &= \underbrace{\frac{\omega^2 \left|\tilde{Q}^M\right|^2}{8\pi\rho_0 c_0}}_{W_0} \underbrace{\frac{(M_\infty^2 - 4 + 4\sqrt{1-M_\infty^2})\pi}{4M_\infty (1-M_\infty^2)^{5/2}}}_{\sigma_2} \end{aligned} \tag{37}$$

$$\begin{aligned} W_{M_\infty,3} &= \frac{\omega^2 \left|\tilde{Q}^M\right|^2 r^2}{16\pi\rho_0 c_0} \int_0^\pi \frac{M_{\infty R}\hat{R}_i \hat{r}_i}{R^{*2}} \sin\theta d\theta \\ &= \underbrace{\frac{\omega^2 \left|\tilde{Q}^M\right|^2}{8\pi\rho_0 c_0}}_{W_0} \underbrace{\frac{M_\infty - (1+M_\infty^2)\,\mathrm{arctanh}[M_\infty]}{M_\infty (1-M_\infty^2)^2}}_{\sigma_3} \end{aligned} \tag{38}$$

$$\begin{aligned} W_{M_\infty,4} &= \frac{\omega^2 \left|\tilde{Q}^M\right|^2 r^2}{16\pi\rho_0 c_0} \int_0^\pi \frac{(1-M_{\infty R})M_{\infty R}}{R^{*2}} M_\infty \sin^2\theta d\theta \\ &= \underbrace{\frac{\omega^2 \left|\tilde{Q}^M\right|^2}{8\pi\rho_0 c_0}}_{W_0} \underbrace{\frac{(2(-1+\sqrt{1-M_\infty^2}) + M_\infty^2(-1+2\sqrt{1-M_\infty^2}))\pi}{4M_\infty (1-M_\infty^2)^{5/2}}}_{\sigma_4} \end{aligned} \tag{39}$$

where is W_0 the acoustic power output from a stationary monopole point source in the quiescent acoustic medium; $\sigma_n, n = 1,2,3,4$ represents the component of the APR contributed from the *n*th term in Eq. (15). Substituting Eqs. (36)-(39) into Eq. (32), we can obtain the APR for the monopole source as follows

$$\sigma_T = \sum_{n=1}^{4} \sigma_n = \frac{-\pi + \pi \Big/ \sqrt{1-M_\infty^2} + 2\,\mathrm{arctanh}[M_\infty]}{2M_\infty(1-M_\infty^2)} \tag{40}$$

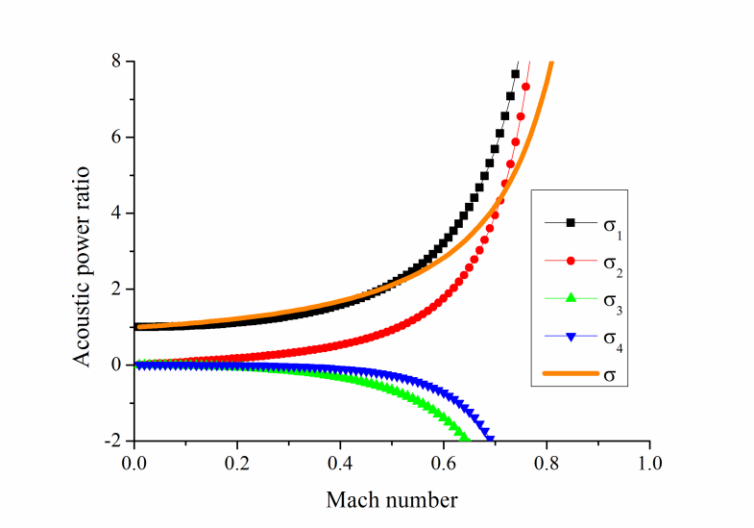

Fig. 14 Effect of the flow Mach number on the acoustic power ratio for the stationary monopole point source

Fig. 14 displays the variation of the APR with the Mach number of the uniform mean flow. The curves display that, at the limit of the Mach number approaching zero, σ_1 approaches one and the other three terms approach zero. This feature is consistent with the analytical result obtained from Eq. (15). The result also indicates that, at a low-Mach-number flow, the contribution from the last three terms in Eq. (15) is much smaller than that from the first term, implying that the uniform mean flow has an ignorable effect on the acoustic power output. However, when the Mach number gradually increases, ignoring the convective effect will cause a large computational error of the acoustic power. Note that the APR approaches infinity when the Mach number of uniform mean flow approaches one.

It is interesting that the first two terms σ_1 and σ_2 have positive contributions to the overall acoustic power, whereas the last two terms σ_3 and σ_4, both of which contain the inner product of the acoustic velocity vector and the Mach number vector, have negative contributions to the overall acoustic power, i.e., absorbing acoustic energy output from the first two terms. This feature could be explained by the computational result shown in Fig. 1. The convective amplification makes the acoustic pressure and the acoustic velocity upstream the source always be higher than those downstream. For observers upstream of the source, the inclined angle between the acoustic velocity

vector and the Mach number vector of the uniform mean flow is larger than 90°, causing the real part of $\tilde{\mathbf{u}}'^{\dagger}\cdot\mathbf{M}_{\infty}$ be negative, whereas the inclined angle is smaller than 90° for the observer downstream the source, causing the real part of $\tilde{\mathbf{u}}'^{\dagger}\cdot\mathbf{M}_{\infty}$ be positive. Therefore, the surface integral over the last two terms σ_3 and σ_4 output a negative acoustic power. Similarly, the convective amplification can be used to explain the reason for the first two terms σ_1 and σ_2 outputting a positive acoustic power.

We revisit the work of Ffowcs Williams and Lovely [21], who concluded that the APR for the monopole source can be approximately expressed by (Eq. 10 in [21])

$$\sigma = 1+5M^2+O(M^4) \tag{41}$$

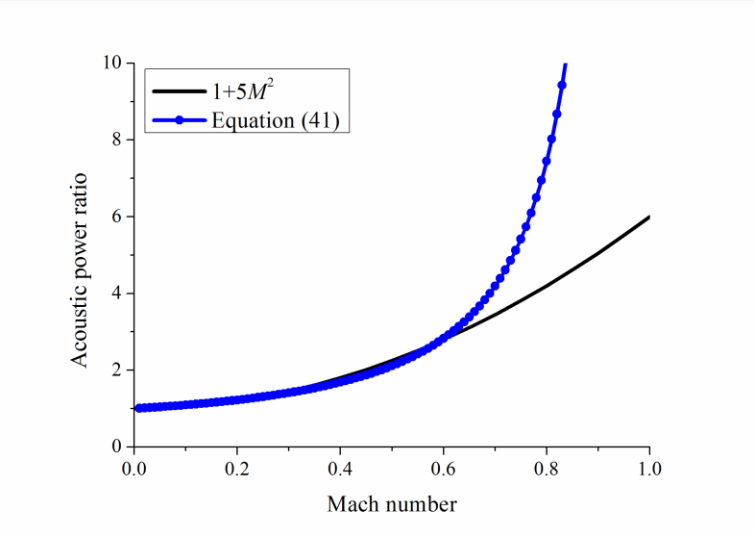

Fig. 15 Comparison between the result obtained from Eq. (40) with that from Eq. (41)

Fig. 15 compares the computational result obtained in this paper and that given in [21], showing a reasonable consistency between these two results for Mach number lower than 0.6. However, an obvious deviation exists with the further increase of the Mach number. Therefore, Eq. (41) only gives an approximate correction of the acoustic power output suitable for a low-Mach-number flow, and this paper presents an analytical correction for the whole region of subsonic flow.

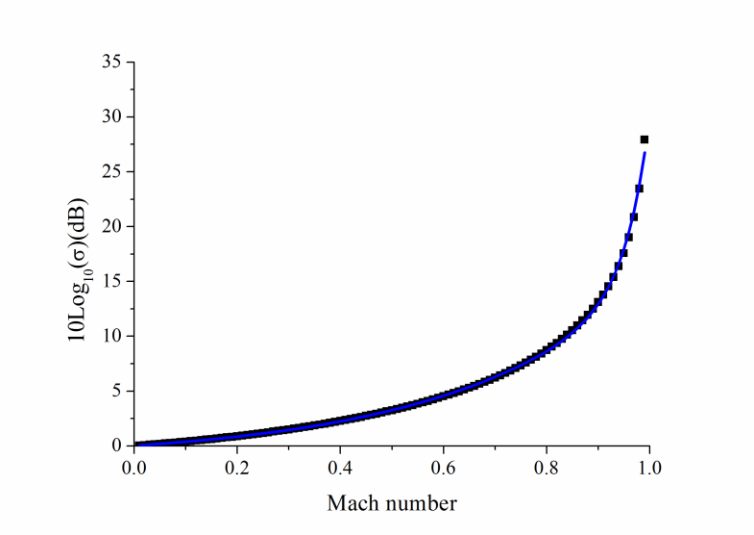

Fig. 16 Correction of the acoustic power level

Furthermore, we consider the correction of the acoustic power level caused by the APR. Fig. 16 indicates that, at the Mach number of 0.7, the correction of the acoustic power level is up to 6dB. Therefore, it is necessary to account for this effect on the acoustic power output in a high-Mach-number flow. A fitting curve of the acoustic power level correction shown in Fig. 16 is described as follows:

$$10\log_{10}(\sigma) \approx -1.22012 + 2.68272\times10^{-9} e^{M_\infty/0.04439} + 1.24383 e^{M_\infty/0.38887}, M_\infty \in [0.01, 0.99] \tag{42}$$

D. Comparison of acoustic power output

In this subsection, we analyze the acoustic power output in two cases. The first is a uniformly moving source in a quiescent acoustic medium, and the second is a stationary source in a uniform mean flow. The source strength is exactly the same in these two cases, and the acoustic power output from the monopole and dipole sources is studied, respectively.

In the first case, Tanna and Morfey [23] deduced the APR for the monopole point source as follows

$$\sigma = \frac{1}{\left(1 - M_\infty^2\right)^2} \tag{43}$$

Morfey and Tanna [19] also deduced the following two equations for the dipole point source whose axis is parallel and perpendicular to the mean flow direction, respectively.

$$\sigma = \frac{3}{2M_\infty^3}\left[\frac{2M(2M_\infty^2-1)}{\left(1-M_\infty^2\right)^2}+\ln\left(\frac{1+M_\infty}{1-M_\infty}\right)\right] \tag{44}$$

$$\sigma = \frac{3}{2M_\infty^3}\left[\frac{M}{1-M_\infty^2}-\frac{1}{2}\ln\left(\frac{1+M_\infty}{1-M_\infty}\right)\right] \tag{45}$$

As shown in Fig. 17, the computational result obtained from Eq. (40) is not the same as that from Eq. (43), but these two curves fit well with each other in the whole subsonic region. Therefore, the time-space transformation techniques mentioned in Section I can be used to calculate the acoustic power output from the monopole source, and the deviation is ignorable even at high Mach numbers.

As analyzed in Section II and Section IV.B, the acoustic power output from a dipole source is non-conservative in the uniform mean flow and it is dependent on the Helmholtz number. Therefore, we compute numerically the APR in the cases of He=0.03, 0.3 and 3.0, respectively. The numerical result is compared with the analytical APR for a moving dipole source in the quiescent acoustic medium, as shown in Fig. 18. The APRs of the two cases are nearly the same in low Mach numbers, but there is a serious deviation between these two APRs when the Mach number is higher than 0.7, especially for the dipole source whose axis is perpendicular to the mean flow direction. Therefore, time-space transformation techniques are only valid for calculating the acoustic power output from a dipole source in the case of low Mach numbers, such as noise generated from high-speed trains, but they cannot be used in the case of high Mach numbers.

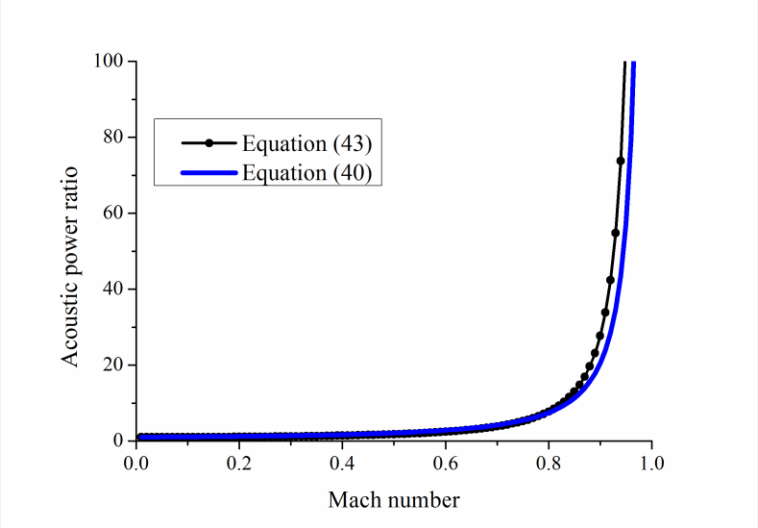

Fig. 17 Comparison of acoustic power ratio for a monopole point source

Additionally, the computational results shown in Fig. 18 also indicate that the effect of the Helmholtz number on the acoustic power output from the dipole source becomes insignificant with the increase in the Helmholtz number. This phenomenon implies that the acoustic power output from the dipole source can be approximately regarded be conservative for high frequency sound in acoustic far field, and this conclusion is consistent with that drawn in Section IV.B.

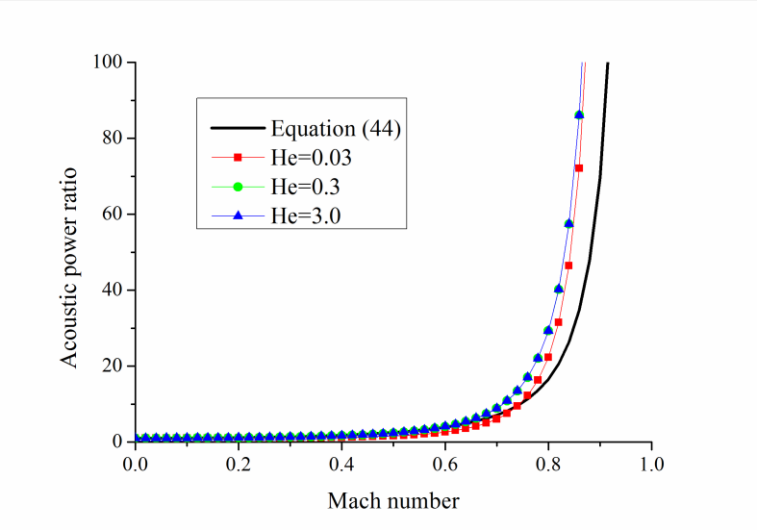

(a)

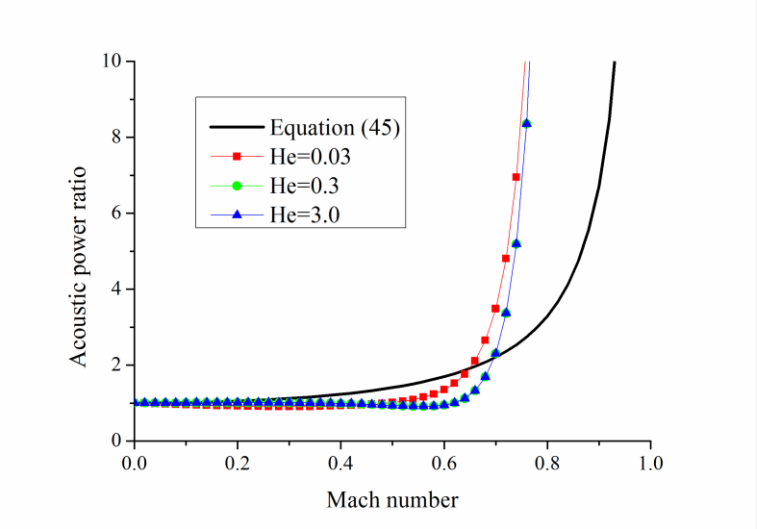

(b)

Fig. 18 Comparison of acoustic power ratio for a dipole point source: (a) dipole axis parallel to the mean flow; (b) dipole axis perpendicular to the mean flow

V. Conclusion

Based on the acoustic pressure and acoustic velocity integral formulations suitable for uniform mean flow, this paper developed a numerical method to compute and visualize the acoustic intensity field around stationary and

rotating sources in a uniform mean flow, which is an extension of the recently developed vector aeroacoustics method with an assumption of quiescent acoustic medium [5, 7]. Moreover, the acoustic power output from the monopole and dipole sources in the uniform mean flow was studied analytically and numerically.

It is widely known that the convective amplification usually makes the direction of the maximum acoustic pressure inclines upstream. In this paper, it is found that the feature of convective amplification also exists for the acoustic velocity field in a uniform mean flow. However, the acoustic intensity fields around the monopole and dipole sources either at rest or in rotation do not satisfy the feature of the convective amplification, and the directivity pattern of the acoustic intensity highly depends on the source type and the mean Mach number. For the stationary or rotating monopole source, the upstream acoustic intensity field is always symmetric to the downstream acoustic intensity field, implying that the acoustic power radiated to the upstream direction is equal to that radiated to the downstream direction. Moreover, the percentage of the acoustic energy concentrating on the plane perpendicular to the direction of uniform mean flow increases with the Mach number of uniform mean flow. For the dipole source in a uniform mean flow, the acoustic intensity is usually asymmetric, and the direction of the maximum acoustic intensity varies with the dipole axis and the mean flow Mach number.

The classic exponent law of the acoustic power output from stationary compact sources, which is obtained with an assumption of quiescent acoustic medium, is only approximately valid for a low-Mach-number flow. In this paper, the effect of uniform mean flow on the acoustic power output from the monopole and dipole sources was studied analytically and numerically. Analytical result shows that the acoustic power output from the monopole source is always conservative, but the acoustic power output from the dipole source is non-conservative in the uniform mean flow, because the acoustic and vortical waves simultaneously stimulated from the dipole source have an energy conversion. Numerical results validate this conclusion and further show that the energy conversion between the acoustic wave and the vortical wave gradually becomes insignificant with the increase in the Helmholtz number. Analytical acoustic power formulation for a stationary monopole point source in the uniform mean flow is derived as well to analyze the effect of Mach number on the acoustic power output. Analytical formulation shows that the approximate result of Ffowcs Williams and Lovely [21] is only suitable for the Mach number smaller than 0.6. Time-space transformation techniques are suitable for calculating the acoustic power output from the monopole source, and these techniques are also approximately valid for the dipole source moving at low Mach numbers, but cannot be used in the case of high Mach numbers.

For aerodynamic noise generated from realistic configurations in moving fluid, such as airframe noise and fan noise, a numerical integral can be performed to compute the acoustic power output by employing the developed acoustic pressure and acoustic velocity formulations for sources in a uniform mean flow. Moreover, the convective vector wave equations of acoustic and vortical waves [15] could be used to analyze waves scattered by solid surfaces in uniform mean flow, and detailed investigations on this topic will be reported in future.

Acknowledgments

The research is supported by the National Natural Science Foundation of China (No. 51476123, No. 51511130075) and Newton Fund (No. IE141516).

References

[1] Lighthill, M. J. "On sound generated aerodynamically. II. Turbulence as a source of sound," *Proceedings of the Royal Society of London A: Mathematical and Physical Sciences* Vol. 222, No. 1148, 1954, pp. 1-32.
doi: 10.1098/rspa.1954.0049

[2] Curle, N. "The influence of solid boundaries upon aerodynamic sound," *Proceedings of the Royal Society of London A: Mathematical And Physical Sciences* Vol. 231, No. 1187, 1955, pp. 505-514.
doi: 10.1098/rspa.1955.0191

[3] Ffowcs Williams, J., and Hawkings, D. "Sound generation by turbulence and surfaces in arbitrary motion," *Philosophical Transactions of the Royal Society of London A: Mathematical, Physical and Engineering Sciences* Vol. 264, No. 1151, 1969, pp. 321-342.
doi: 10.1098/rsta.1969.0031

[4] Goldstein, M. E. *Aeroacoustics*. New York: McGraw-Hill International Book Company, 1976.

[5] Mao, Y., Xu, C., and Qi, D. "Computation of instantaneous and time-averaged active acoustic intensity field around rotating source," *Journal of Sound and Vibration* Vol. 337, 2015, pp. 95-115.
doi: 10.1016/j.jsv.2014.10.023

[6] Lee, S., Brentner, K. S., and Morris, P. J. "Assessment of time-domain equivalent source method for acoustic scattering," *AIAA Journal* Vol. 49, No. 9, 2011, pp. 1897-1906.
doi: 10.2514/1.J050736

[7] Mao, Y., Cai, J., Gu, Y., and Qi, D. "Direct evaluation of acoustic intensity vector field around impedance scattering body," *AIAA Journal* Vol. 53, No. 5, 2015, pp. 1362-1371.
doi: 10.2514/1.J053431

[8] Cantrell, R., and Hart, R. "Interaction between sound and flow in acoustic cavities: mass, momentum, and energy considerations," *The Journal of the Acoustical Society of America* Vol. 36, No. 4, 1964, pp. 697-706.
doi: 10.1121/1.1919047

[9] Morfey, C. L. "Acoustic energy in non-uniform flows," *Journal of Sound and Vibration* Vol. 14, No. 2, 1971, pp. 159-170.
doi: 10.1016/0022-460x(71)90381-6

[10] Myers, M. "An exact energy corollary for homentropic flow," *Journal of Sound and Vibration* Vol. 109, No. 2, 1986, pp. 277-284.

doi: 10.1016/S0022-460X(86)80008-6

[11] Myers, M. K. "Transport of energy by disturbances in arbitrary steady flows," *Journal of Fluid Mechanics* Vol. 226, 1991, pp. 383-400.
doi: 10.1016/S0022-460X(86)80008-6

[12] Atassi, O. V. "Computing the sound power in non-uniform flow," *Journal of Sound and Vibration* Vol. 266, No. 1, 2003, pp. 75-92.
doi: 10.1016/S0022-460X(02)01448-7

[13] Gregory, A. L., Sinayoko, S., Agarwal, A., and Lasenby, J. "An acoustic space-time and the Lorentz transformation in aeroacoustics," *International Journal of Aeroacoustics* Vol. 14, No. 7, 2015, pp. 977-1003.
doi: 10.1260/1475-472X.14.7.977

[14] Rienstra, S. W., and Hirschberg, A. "An introduction to acoustics." 2017. https://www.win.tue.nl/~sjoerdr/papers/boek.pdf

[15] Mao, Y., Hu, Z., Xu, C., and Ghorbaniasl, G. "Vector Aeroacoustics for a uniform mean flow: acoustic velocity and vortical velocity ", 2017. *AIAA Journal*. Revision Submitted.

[16] Xu, C., Mao, Y., and Qi, D. "Frequency-domain acoustic pressure formulation for rotating source in uniform subsonic inflow with arbitrary direction," *Journal of Sound and Vibration* Vol. 333, 2014, pp. 3081-3091.
doi: 10.1016/j.jsv.2014.03.004

[17] Waterhouse, R. V., Yates, T. W., Feit, D., and Liu, Y. N. "Energy streamlines of a sound source," *Journal of the Acoustical Society of America* Vol. 78, No. 2, 1985, pp. 758-762.
doi: 10.1121/1.392445

[18] Waterhouse, R. V., and Feit, D. "Equal-energy streamlines," *Journal of the Acoustical Society of America* Vol. 80, No. 2, 1986, pp. 681-684.
doi: 10.1121/1.394064

[19] Morfey, C. L., and Tanna, H. K. "Sound radiation from a point force in circular motion," *Journal of Sound and Vibration* Vol. 15, No. 3, 1971, pp. 325-351.
doi: 10.1016/0022-460x(71)90428-7

[20] Mao, Y., and Xu, C. "Analytical acoustic power spectrum formulations for rotating monopole and dipole point sources," *Journal of Vibration and Acoustics* Vol. 138, No. 2, 2016, p. 021009.
doi: 10.1115/1.4032139

[21] Ffowcs Williams, J., and Lovely, D. "Sound radiation into uniformly flowing fluid by compact surface vibration," *Journal of Fluid Mechanics* Vol. 71, No. 04, 1975, pp. 689-700.
doi: 10.1017/S0022112075002790

[22] Dowling, A. "Convective amplification of real simple sources," *Journal of Fluid Mechanics* Vol. 74, No. 03, 1976, pp. 529-546.
doi: 10.1017/S0022112076001936

[23] Tanna, H. K., and Morfey, C. L. "Sound radiation from point sources in circular motion," *Journal of Sound and Vibration* Vol. 16, No. 3, 1971, pp. 337-348.
doi: 10.1016/0022-460x(71)90591-8